IEICE TRANS. ELECTRON., VOL.E99–C, NO.1 JANUARY 2016

PAPER Special Section on Recent Progress in Electromagnetic Theory and Its Application

Numerical Study on Path Loss Characteristics Considering Antenna Positions on Car Body at Blind Intersection in Urban Area for Inter-Vehicle Communications Using 700 MHz Band

Suguru IMAI[†a)], **Kenji TAGUCHI**[†], *Members*, **Takeshi KAWAMURA**[†], *Nonmember*, *and* **Tatsuya KASHIWA**[†], *Senior Member*

SUMMARY In the development of inter-vehicle communication systems for the prevention of car crashes, it is important to know radio propagation characteristics at blind intersections. In field experiments and numerical simulations to investigate radio propagation characteristics, a half wavelength dipole antenna is assumed to be the wave source in many cases. However, a directivity of car antenna is changed by the effect of both car body and antenna position on car. In this paper, path loss characteristics considering antenna positions on car body at a blind intersection in urban area for inter-vehicle communications using 700 MHz band are investigated. Additionally, simplified car models are proposed for the efficient analysis of radio propagation. Here, the hybrid method using both FDTD and ray-tracing methods is used for the radio propagation analysis.

key words: *inter-vehicle communication, blind intersection, car antenna position, radio wave propagation, 760 MHz*

1. Introduction

Recently, collision avoidance systems have been widely used for the prevention of car crashes. Millimeter-wave radar, video camera, and other devices are utilized in these systems. However, it seems that existing systems are difficult to prevent crossing collisions at blind intersections, because it is difficult to detect the car located in the non-line-of-sight region at blind intersections by using existing systems.

On the other hand, inter-vehicle communication systems for the prevention of car crashes have been proposed [1]–[4]. In Europe and the United States, 5 GHz band has been allocated for this system [1], [2]. In Japan, 700 MHz band has been allocated [3], [4]. Car accidents at blind intersections can be prevented by sending and receiving information such as the location and speed of vehicle by using these systems. In the development of inter-vehicle communication systems, it is important to know characteristics of radio wave propagation at blind intersections. Hence, field experiments and numerical simulations have been performed to investigate radio propagation characteristics [5]–[7].

By the way, a half wavelength dipole antenna as a reference antenna is assumed to be the wave source in many experiments and simulations. However, a directivity of car antenna is changed by the effect of both car body and antenna position on car. Therefore, it is important to investigate the effect of car antenna position on radio propagation characteristics. In terms of the design of car exterior, it is also important to clarify the relationship between antenna positions and propagation characteristics. Traditionally, in [8]–[10], the effect of car antenna positions on radio propagation characteristics for 5 GHz band has been investigated. However, these characteristics not well known for 700 MHz band used in Japan. Therefore, we have investigated the effect of car antenna positions for 700 MHz band [11]. Additionally, it seems important to know the ray cluster of arrival direction of received wave in order to clarify the multipath environment in blind intersection. And, in between sending and receiving cars, it seems necessary to investigate the propagation characteristics for not only same height but also different height in terms of antenna positions on car body. Also, it would be needed to know the effect of different car locations at an intersection.

In this paper, path loss characteristics considering antenna positions on car body at a blind intersection in urban area for inter-vehicle communications using 700 MHz band are investigated in terms of the follows:

- simplified car models for the efficient analysis of path loss characteristics,
- the effect of car antenna positions on path loss,
- a comparison of path loss for car antenna and $\lambda/2$ vertical dipole antenna,
- the effect of receiving height and car location at intersection on path loss,
- the ray cluster at receiving point in the non-line-of-sight region.

Here, the hybrid method using both FDTD and ray-tracing methods is used for the radio propagation analysis [12].

2. Blind Intersection in Urban Area and Car Model

Figure 1 shows a blind intersection in urban area. Table 1 shows parameters used in this paper. In this work, the case of narrow width of road is considered as an example. A height of buildings is approximated by infinity, because it seems that the effect of diffraction waves over the top of

Manuscript received April 9, 2015.
Manuscript revised August 4, 2015.
[†]The authors are with the Department of Electrical and Electronic Engineering, Kitami Institute of Technology, Kitami-shi, 090–8507 Japan.
a) E-mail: now_i@mail.kitami-it.ac.jp
DOI: 10.1587/transele.E99.C.36

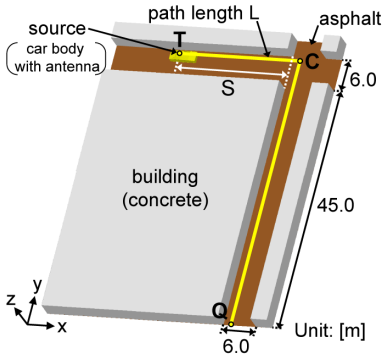

Fig. 1 Blind intersection in urban area.

Table 1 Parameters used in this paper

frequency	760 MHz
car location	S = 10, 20, 30 m
receiving height	h = 0.405, 1.5 m
road (dry asphalt) [13]	ε_r = 4.9, σ = 0.00761 S/m
building (concrete) [14]	ε_r = 7.0, σ = 0.0473 S/m

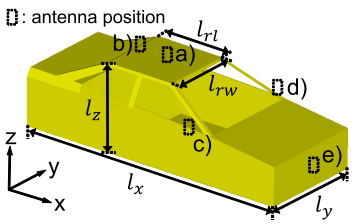

Fig. 2 Car model and antenna positions: a) rooftop center, b) rooftop rear, c) right door mirror, d) left door mirror, e) front bumper. Here, l_x = 4.64 m, l_y = 1.76 m, l_z = 1.3 m, l_{rl} = 1.2 m, l_{rw} = 1.2 m.

building is sufficiently small for the inter-vehicle communications at the intersection in urban area. It is assumed that the road and buildings consist of asphalt and concrete, respectively. Car location S shows the distance of intersection to car. Cases of S = 10, 20, 30 m are investigated. These values correspond to the stopping distance of car for about 30, 40, 50 km/h, respectively [15]. The line TCQ indicates a path to calculate a path loss at a blind intersection. This path is set considering the prevention of car crashes at point C. Here, it is assumed that the car rooftop center is located at the point T in the blind intersection. The transparent wave from buildings is not considered, that is, it is assumed that a thickness of building wall is infinity. The reason why is that it is important to know the worst case of path loss at a blind intersection in urban area.

Figure 2 shows a car model and antenna positions. In this paper, a small sedan type that is typically used in Japan is selected as an example. It is assumed that a car body is composed of the perfect electric conductor. Five kinds of antenna positions are investigated as examples. The reasons are that the rooftop is widely used to mount a car antenna at present, and that positions of door mirror and bumper seem to be able to cover the antenna so that it is not visible externally.

Table 2 Antenna type used in this paper

reference antenna		$\lambda/2$ vertical dipole antenna
car antenna	rooftop center, rooftop rear	$\lambda/4$ vertical monopole antenna
	right door mirror, left door mirror, front bumper	$\lambda/2$ vertical dipole antenna

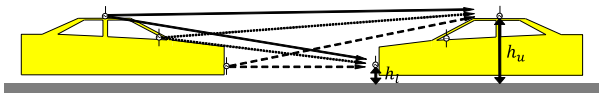

Fig. 3 Upper and lower bounds of receiving height h for car model used in this paper: upper bound h_u = 1.5 m, lower bound h_l = 0.405 m.

Table 2 shows the antenna type used in this paper. In this work, a vertical antenna is used because the use of vertical polarization is recommended for the inter-vehicle communications in Japan [3]. In fact, a normal mode helical antenna has been used in a rooftop of actual car [16]. However, the directivity of this antenna is similar to one of monopole antenna. Therefore, in this paper, a monopole antenna has been used in terms of a simple modeling in the numerical simulation.

Figure 3 shows the upper and lower bounds of the receiving height h for the car model used in this paper. As shown in this figure, we consider the upper and lower bounds of height of antenna positions that are able to mount on car body. The upper bound becomes h_u = 1.5 m and the lower bound is h_l = 0.405 m in this model. The path loss in the receiving height h corresponding to these bounds for a car antenna position on the sending car should be investigated. Here, the car body and antenna in receiving point are not considered in this work.

3. Hybrid Method for Radio Propagation Analysis

In a large scale analysis like a radio propagation analysis at an intersection in urban area, the ray-tracing method is widely used. However, this method has a disadvantage that is increased the computational effort by dealing with objects of complex shape such as a car body. On the other hand, in the large scale analysis used the FDTD method, there is a disadvantage that requires a large memory. Therefore, in this paper, it seems that the hybrid method using both FDTD and ray-tracing methods is useful [12].

Figure 4 shows a procedure of hybrid method for radio propagation analysis using both FDTD and ray-tracing methods: 1) the electromagnetic analysis for car antenna mounted on a car is performed by using the FDTD method, 2) the directivity is calculated by using FDTD results and the equivalence theorem, 3) radio propagation characteristics at intersection are calculated by using the ray-tracing method with the directivity obtained by 2). Table 3 shows simulation conditions used in this paper.

In this work, the car antenna mounted on car body is located near the ground and building wall in the intersection.

The directivity under these conditions might be changed compared with that located in the free space by the interaction among a car body with antenna, ground and building walls. However, in this paper, it is assumed that the effects of interaction are small. Figure 5 shows the comparison of path loss obtained by FDTD and hybrid methods in case of rooftop center at blind intersection. Here, the case of $S = 20$ m and $h = 1.5$ m is shown as an example. As shown in this figure, it is seen that the path loss obtained by using the hybrid method agree with that obtained by the FDTD full-wave analysis of the blind intersection considering car body with antenna. Therefore, it seems that this assumption is reasonable.

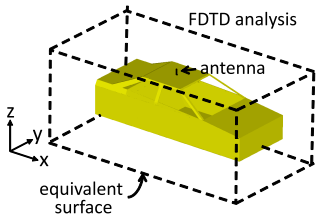

1) Electromagnetic analysis of car antenna.

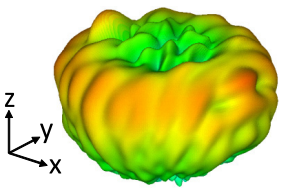

2) Calculation of directivity by using equivalence theorem.

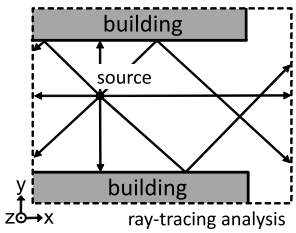

3) Radio propagation analysis at intersection in urban area.

Fig. 4 Procedure of hybrid method for radio propagation analysis using both FDTD and ray-tracing methods.

Table 3 Simulation conditions

FDTD method	spatial increment	1.0 cm
ray-tracing method	maximum number of reflection	10
	maximum number of diffraction	1
	diffraction coefficient	UTD method [17]

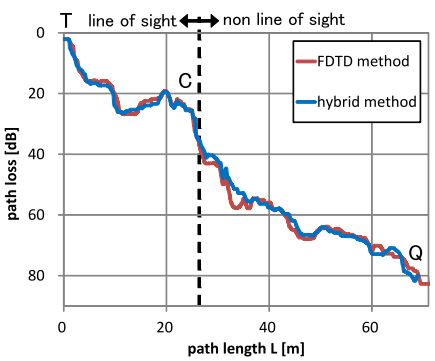

Fig. 5 Comparison of path loss obtained by FDTD and hybrid methods in case of rooftop center at blind intersection ($S = 20$ m, $h = 1.5$ m, $|E_z|$ component, strict model).

4. Simplified Car Model for Efficient Analysis of Radio Propagation

The modeling of complex shape such as car body is a cumbersome task. Therefore, in this section, a simplified car model for efficient analysis of radio propagation is proposed.

It seems that currents on car body become strong at vicinity of antenna position. Therefore, it is considered that a strict car model can be simplified to the metallic plate of vicinity of antenna position. However, it seems that an optimal simplified model is different for each antenna position.

Figures 6, 7 and 8 show simplified car models for each antenna position considered in this paper. These simplified car models are easy to modeling compared with strict car models.

4.1 Current Distribution and Directivity

Figures 9, 10, 11 and 12 show the current distribution and directivity for strict and simplified car models. Here, in this paper, cases of rooftop center and right door mirror are shown as examples. And, current distributions are normalized so that a radiation power becomes 1 W.

As shown in Figs. 9 (a) and 10 (a), it seems that the current distribution on rooftop panel for the simplified model indicates the same tendency as that for the strict model. On the other hand, it is shown that the current on the bonnet,

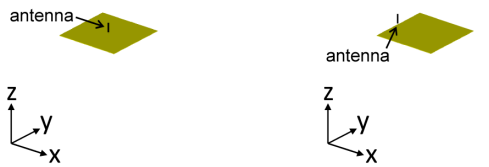

(a) rooftop center (b) rooftop rear

Fig. 6 Simplified car models in case of rooftop.

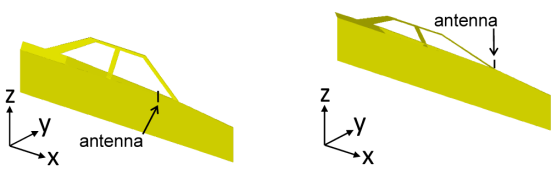

(a) right door mirror (b) left door mirror

Fig. 7 Simplified car models in case of door mirror.

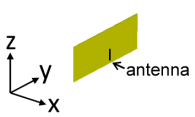

Fig. 8 Simplified car models in case of front bumper.

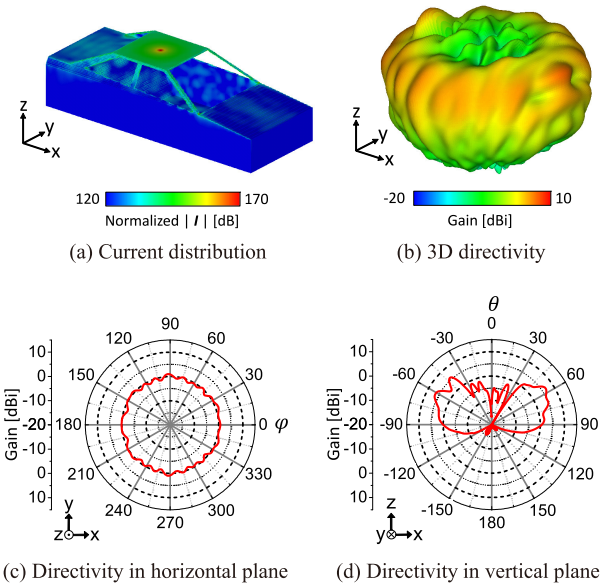

(a) Current distribution (b) 3D directivity

(c) Directivity in horizontal plane (d) Directivity in vertical plane

Fig. 9 Current distribution and directivity for strict car model in case of rooftop center.

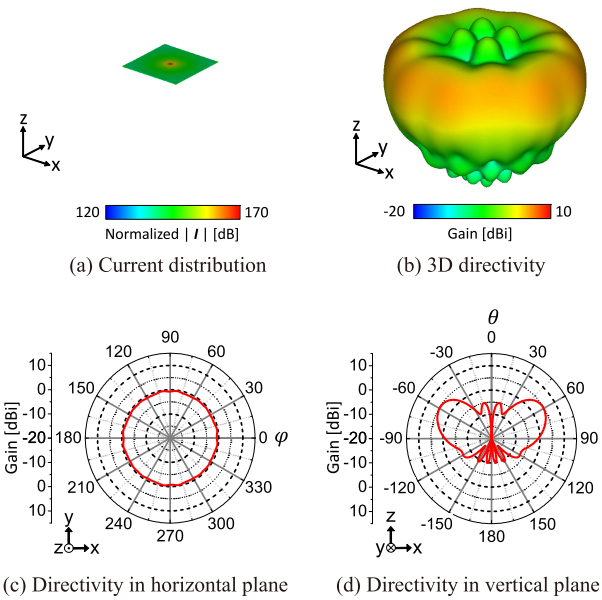

(a) Current distribution (b) 3D directivity

(c) Directivity in horizontal plane (d) Directivity in vertical plane

Fig. 10 Current distribution and directivity for simplified car model in case of rooftop center.

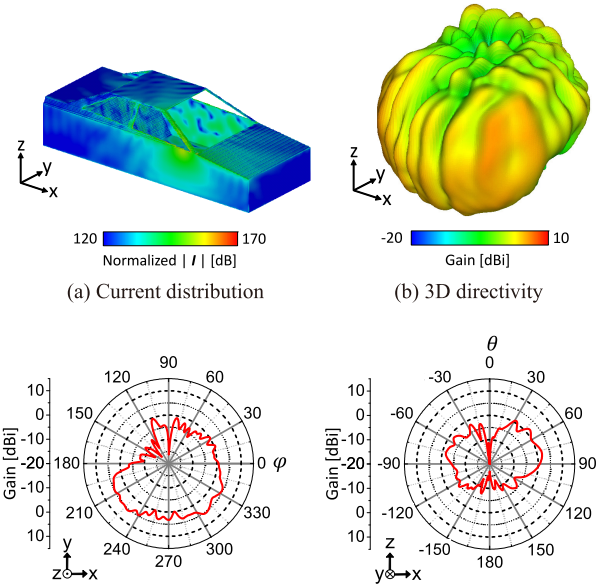

(a) Current distribution (b) 3D directivity

(c) Directivity in horizontal plane (d) Directivity in vertical plane

Fig. 11 Current distribution and directivity for strict car model in case of right door mirror.

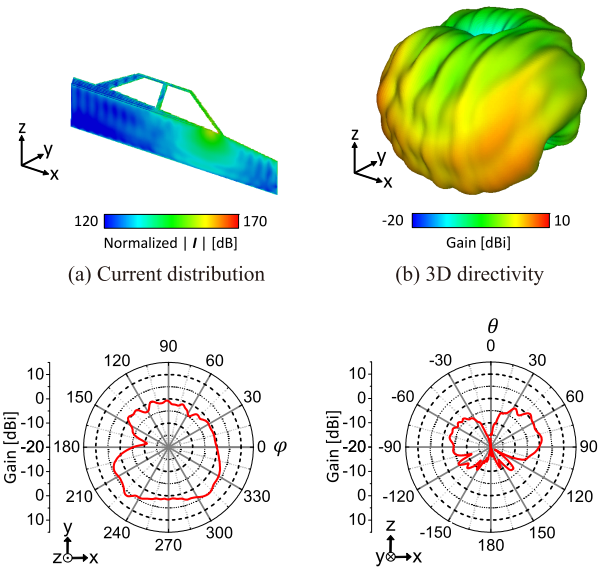

(a) Current distribution (b) 3D directivity

(c) Directivity in horizontal plane (d) Directivity in vertical plane

Fig. 12 Current distribution and directivity for simplified car models in case of right door mirror.

trunk and inside of car seem relatively strong for the strict model. In Figs. 9 (b) to 9 (d), and Figs. 10 (b) to 10 (d), it is seen that the radiation pattern for the simplified model denotes the same tendency as that for the strict model. However, it seems that a roughness of radiation pattern for the simplified model is small compared with that for the strict model.

In Figs. 11 and 12, it is seen that current distributions on right side panel of car denote the same tendency for both strict and simplified models. However, in the strict model, it is indicated that the current on the bonnet and so on are strong relatively. On the other hand, it seems that radiation patterns are similar in between strict and simplified car models except for its roughness.

4.2 Comparison of Path Loss for Strict and Simplified Car Models

Figure 13 shows the comparison of path loss for strict and simplified car models at a blind intersection. Here, cases of rooftop center and right door mirror are shown for the case

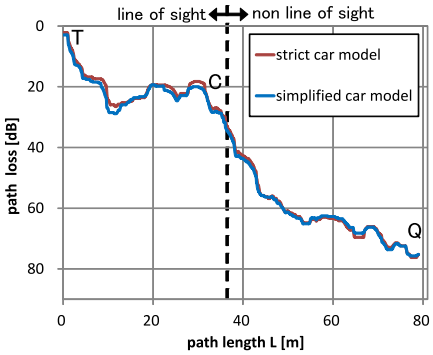

(a) rooftop center

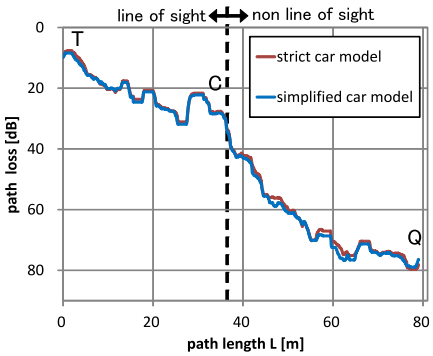

(b) right door mirror

Fig. 13 Comparison of path loss for strict and simplified car models at blind intersection ($S = 30$ m, $h = 1.5$ m, $|E_z|$ component).

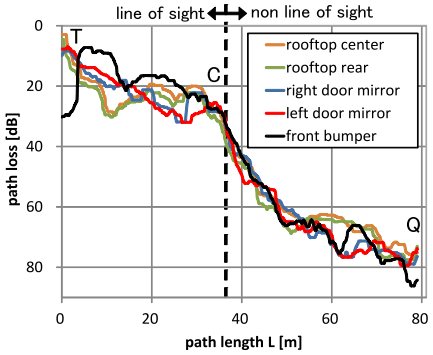

Fig. 14 Path loss for each antenna position at blind intersection ($S = 30$ m, $h = 1.5$ m, $|E_z|$ component, simplified model).

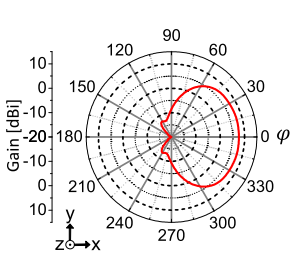

(a) Horizontal plane

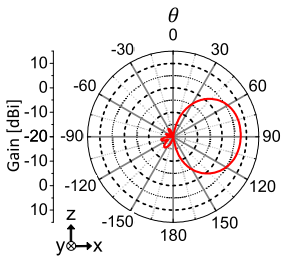

(b) Vertical plane

Fig. 15 Directivity for simplified car model in case of front bumper.

of $S = 30$ m and $h = 1.5$ m as examples. In this paper, the path loss indicates the median value within interval of 4 m along the TCQ path [7]. Also, the path loss for $|E_z|$ component is denoted, because the vertical polarization is used for inter-vehicle communications in Japan.

As shown in this figure, it is seen that the path losses for simplified model are quantitatively similar to that for the strict model. Although cases of other antenna positions are not shown in this paper due to limitations of space, it can be seen that the same tendency is indicated. And we confirmed that the computational time and memory usage for the FDTD analysis used simplified car models become one-fifth to one-half of the case of strict car model. As a result, it is shown that the simplified car model can be used in the efficient analysis of path loss at a blind intersection. In Sect. 5, simplified car models are used.

5. Path Loss at Blind Intersection in Urban Area

5.1 Effect of Car Antenna Positions on Path Loss

Figure 14 shows the path loss for each antenna position at a blind intersection in urban area. Here, the case of $S = 30$ m and $h = 1.5$ m is shown as an example.

As shown in this figure, it is seen that path losses differ quantitatively for each antenna position. However, it seems that path losses for each antenna position indicate the qualitatively same tendency for each other. Here, in the case of front bumper, it is seen that the path loss in range of $L < 3$ m increased about 20 dB. This reason is from as follows. In this work, the point T is located at the left side of front bumper. Additionally, as shown in Fig. 15, it is seen that the radiation of radio wave is slightly in the left side of front bumper. Therefore, the path loss at vicinity of point T becomes large. Although other cases are not shown in this paper, in cases of $S = 10$, 20 m and $h = 0.405$ m, it is seen that path losses for each antenna position denote the qualitatively same tendency for each other.

5.2 Comparison of Path Loss for Car Antenna and $\lambda/2$ Vertical Dipole Antenna

Figure 16 shows the comparison of path loss for car antenna and $\lambda/2$ vertical dipole antenna at blind intersection in urban area. Here, cases of rooftop center, right door mirror and front bumper are shown for the case of $S = 30$ m and $h = 1.5$ m as examples. In this paper, it considers that $\lambda/2$ vertical dipole antenna is located in each antenna position without car body.

As shown in this figure, it seems that path losses for car antenna denote the same tendency with the case of $\lambda/2$ vertical dipole antenna for the rooftop center, right door mirror and front bumper, respectively. However, it is seen that the path loss for car antenna is quantitatively different compared with that for $\lambda/2$ vertical dipole antenna. The reason is considered that the directivity of car antenna is slightly different in the front side of car compared with that of $\lambda/2$

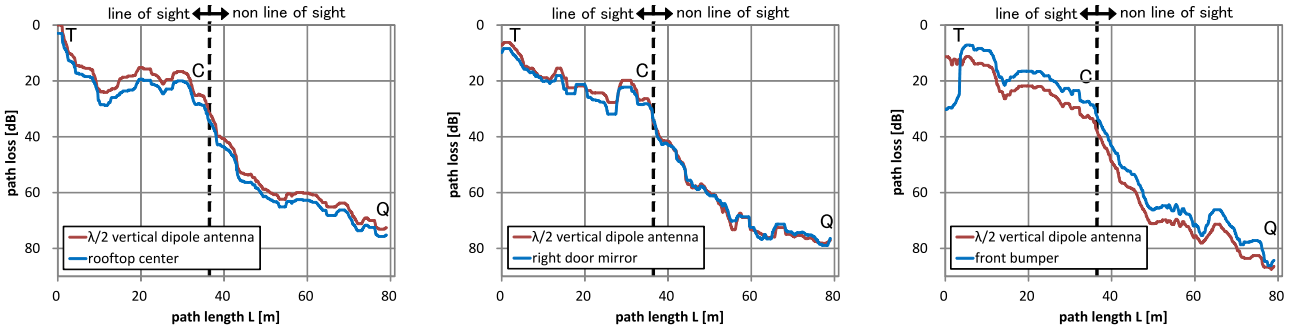

(a) rooftop center (b) right door mirror (c) front bumper

Fig. 16 Comparison of path loss for car antenna and $\lambda/2$ vertical dipole antenna at blind intersection ($S = 30$ m, $h = 1.5$ m, $|E_z|$ component, simplified model).

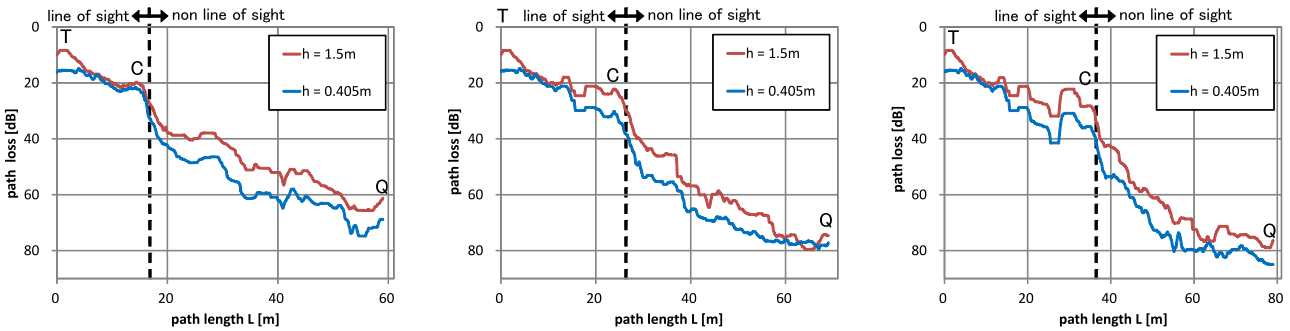

(a) $S = 10$ m (b) $S = 20$ m (c) $S = 30$ m

Fig. 17 Path loss for different receiving height and car location in case of right door mirror at blind intersection ($|E_z|$ component, simplified model).

vertical dipole antenna. For example, it can be seen that the directivity for simplified model of rooftop center in front of car is about 3 dB less than that for $\lambda/2$ vertical dipole antenna as shown in Fig. 10 (c). And, as shown in Figs. 12 (c) and 15 (a), it is seen that the gain at front side of car become about 0.0 dBi and 7.6 dBi for cases of right door mirror and front bumper, respectively. Although other cases are not shown by limitations of space, the same tendency is indicated for other antenna positions. Additionally, it is seen that cases of $S = 10$, 20 m and $h = 0.405$ m are also similar. As a result, it is seen that the path loss can be evaluated qualitatively by using the $\lambda/2$ vertical dipole antenna in this case.

5.3 Effect of Receiving Height and Car Location at Intersection on Path Loss

Figure 17 shows the path loss for the different receiving height and car location at a blind intersection. Here, the case of right door mirror is shown as an example.

As shown in this figure, it is seen that path losses for $h = 1.5$ m decrease compared with that for $h = 0.405$ m in the non-line-of-sight region for cases of $S = 10$, 20 and 30 m. Although cases of other antenna positions are not shown in this paper, it can be seen that the same tendency is indicated for cases of other antenna positions. As a result, it is shown that the path loss for $h = 1.5$ m is smaller than that for $h = 0.405$ m at blind intersection in urban area.

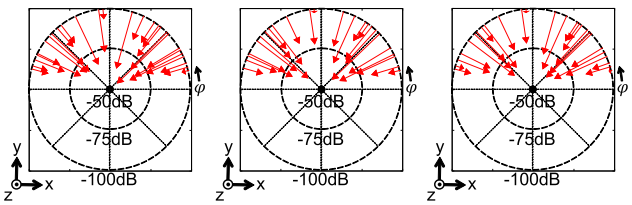

(a) rooftop center (b) right door mirror (c) front bumper

Fig. 18 Ray clusters at $L = 46$ m in non-line-of-sight region of blind intersection ($S = 30$ m, $h = 1.5$ m, $|E_z|$ component, simplified model).

6. Ray Clusters at Receiving Point in Non-Line-of-Sight Region of Blind Intersection

Figures 18, 19 and 20 show the ray cluster at each path length L in non-line-of-sight region of blind intersection, respectively. Here, cases of rooftop center, right door mirror and front bumper are shown for the case of $S = 30$ m and $h = 1.5$ m as examples. And cases of receiving points for path length $L = 46$, 56 and 66 m are investigated as examples. In these figures, directions of $\phi = 0$ and 180 deg. correspond to building walls.

As shown in Fig. 18, it seems that waves coming from

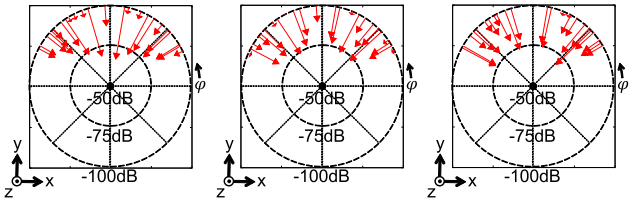

(a) rooftop center (b) right door mirror (c) front bumper

Fig. 19 Ray clusters at $L = 56$ m in non-line-of-sight region of blind intersection ($S = 30$ m, $h = 1.5$ m, $|E_z|$ component, simplified model).

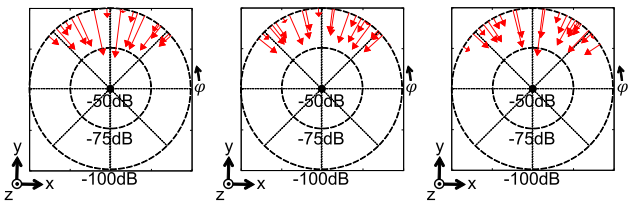

(a) rooftop center (b) right door mirror (c) front bumper

Fig. 20 Ray clusters at $L = 66$ m in non-line-of-sight region of blind intersection ($S = 30$ m, $h = 1.5$ m, $|E_z|$ component, simplified model).

three directions of about 30, 45 and 135 deg. are relatively strong for each antenna position. It is considered that these indicate reflected waves from building walls. On the other hand, by comparison of Figs. 18-20, it is seen that the arrival waves become a similar intensity with each other when increasing the path length. We confirmed that it has the same tendency for other cases of antenna positions, S, and h.

7. Conclusions

In this paper, path loss characteristics considering antenna positions on car body at a blind intersection in urban area for 760 MHz inter-vehicle communications were investigated. And, simplified car models were proposed for the efficient analysis of path loss characteristics. As a result, in the blind intersection in urban area as shown in this paper, the following new knowledge was obtained:

- the simplified car model can be used for the efficient analysis of path loss characteristics,
- the path loss differ quantitatively for each antenna position considered in this study, however, the qualitatively same tendency is indicated,
- the path loss for car antenna indicates the same tendency as that for $\lambda/2$ vertical dipole antenna,
- the path loss for the receiving height $h = 1.5$ m is smaller than that for $h = 0.405$ m with respect to each antenna position in cases of car location $S = 10$, 20 and 30 m,
- the arrival waves from direction of building walls are relatively strong when the receiving point is near the intersection, on the other hand, the arrival waves become a similar intensity with each other when increasing distance from the intersection.

In the near future, the effect of transparent wave from buildings will be investigated to know the radio propagation characteristics in the actual environment that is not a worst case. Additionally, the relationship between the simulation results and the prediction model of path loss such as ITU-R P.1411 [18] will be investigated.

Acknowledgments

This work was supported by JSPS KAKENHI Grant Numbers 26420335 and 24510221.

References

[1] ETSI TR 102 638, "Intelligent transport systems (ITS); vehicular communications; basic set of applications; definitions," v1.1.1, June 2009.
[2] IEEE standard for information technology – Telecommunication and information exchange between systems local and metropolitan area networks – specific requirements part 11: wireless LAN medium access control (MAC) and physical layer (PHY) specifications, IEEE Std. 802.11-2012, March 2012.
[3] ARIB, "700MHz band intelligent transport systems," ARIB STD-T109, version 1.2, Dec. 2013.
[4] ITS Info-communications Forum, "Experimental guideline for vehicle communications system using 700MHz-band," ITS FORUM RC-006 Version 1.0, Feb. 2009.
[5] S. Sai, E. Niwa, K. Mase, M. Nishibori, J. Inoue, M. Obuchi, T. Harada, H. Ito, K. Mizutani, and M. Kizu, "Field evaluation of UHF radio propagation for an ITS safety system in an urban environment," IEEE Commun. Mag., vol.47, no.11, pp.120–127, Nov. 2009.
[6] K. Ito, K. Sanda, M. Takanashi, and Y. Tadokoro, "A study on effect of surrounding vehicles on propagation loss characteristics in inter-vehicle communications," IEICE Trans. Commun. (Japanese Edition), vol.J94-B, no.3, pp.455–467, March 2011.
[7] T. Taga, "Propagation loss model in inter-vehicle communication environments," IEICE Technical Report, A·P2012-145, Jan. 2013.
[8] T. Abbas, J. Karedal, and F. Tufvesson, "Measurement-based analysis: the effect of complementary antennas and diversity on vehicle-to-vehicle communication," IEEE Antennas Wireless Propag. Lett., vol.12, pp.309–312, March 2013.
[9] L. Reichardt, T. Mahler, T. Schipper, and T. Zwick, "Influence of single and multiple antenna placements on the capacity of C2C communication systems," Proc. 43rd European Microwave Conference, EuMC 2013, pp.720–723, Nuremberg, Germany, Oct. 2013.
[10] D. Quack, M. Meuleners, S. Hommen, and C. Degen, "Simulation-based evaluation of MIMO antenna systems in car-to-car communication," in Proceedings of the 8th European Conference on Antennas and Propagation, EuCAP 2014, pp.3049–3052, the Hague, the Netherlands, April 2014.
[11] S. Imai, K. Taguchi, and T. Kashiwa, "Effect of car antenna position on radio propagation characteristics at intersection for 760MHz inter-vehicle communications," in Proceedings of 2014 International Symposium on Antennas and Propagation, ISAP 2014, pp.349–350, Kaohsiung, Taiwan, Dec. 2014.
[12] Y. Wang, S. Safavi-Naeini, and S.K. Chaudhuri, "A hybrid technique based on combining ray tracing and FDTD methods for site-specific modeling of indoor radio wave propagation," IEEE Trans. Antennas Propagat., vol.48, no.5, pp.743–754, May 2000.
[13] E.J. Jaselskis, J. Grigas, and A. Brillingas, "Dielectric properties of asphalt pavement," J. Mater. Civ. Eng., vol.15, no.5, pp.427–434, Oct. 2003.
[14] Rec. ITU-R P.1238-6, "Propagation data and prediction methods for the planning of indoor radiocommunication systems and radio local area networks in the frequency range 900MHz to 100GHz," ITU-R

Recommendations, Oct. 2009.
[15] World Health Organization, Speed management: a road safety manual for decision-makers and practitioners, Geneva: Global Road Safety Partnership, Switzerland, 2008.
[16] J. Ooe and K. Nishikawa, "Overview on vehicle antenna systems," IEICE Trans. Commun. (Japanese Edition), vol.J89-B, no.9, pp.1569–1579, Sept. 2006.
[17] D.N. Schettino, F.J.S. Moreira, K.L. Borges, and C.G. Rego, "Novel heuristic UTD coefficients for the characterization of radio channels," IEEE Trans. Magn., vol.43, no.4, pp.1301–1304, April 2007.
[18] Rec. ITU-R P.1411-7, "Propagation data and prediction methods for the planning of short-range outdoor radiocommunication systems and radio local area networks in the frequency range 300 MHz to 100 GHz," ITU-R Recommendations, Sept. 2013.

Suguru Imai was born in Hokkaido, Japan, on June 23, 1981. He graduated from the Dept. of Computer Science of Kitami Institute of Technology, Japan, in 2005, completed the M.S. and the doctoral programs in 2007 and 2010, respectively. He holds a D.Eng. degree. He became an assistant professor in the Dept. of Electrical and Electronic Eng. of the same university in 2010. He has been engaged in the analysis of electromagnetic fields.

Kenji Taguchi was born in Hokkaido, Japan, on July 2, 1978. He graduated from the Dept. of Electrical and Electronic Eng. of Kitami Institute of Technology, Japan, in 2001, completed the M.S. and the doctoral programs in 2003 and 2006, respectively. He holds a D.Eng. degree. He became a research associate in the Dept. of Info. and Comm. Eng. of Kumamoto National College of Tech. in 2006. He has been an associate professor in the Dept. of Electrical and Electronic Eng. of Kitami Inst. of Tech. since 2009. He has been engaged in the analysis of electromagnetic fields.

Takeshi Kawamura was born in Hokkaido, Japan, in 1962. He received a Bachelor's degree, a Master's degree, and a Ph.D. in precision engineering from Hokkaido University in 1987, 1989, and 2003, respectively. From 1991 to 2003, he worked as a lecturer at the department of Electrical and Electronic Engineering in Kitami Institute of Technology, Hokkaido, Japan. From 2003, he served as an associate professor. He is a member of SICE, ISCIE, IEEJ, RSJ, ITS Japan, and IEEE.

Tatsuya Kashiwa was born in Hokkaido, Japan, on June 3, 1961. He graduated from the Department of Electrical Engineering of Hokkaido University in 1984 and completed the M.S. program in 1986. Before completing the doctoral program, he became a research associate in Department of Electrical Engineering in 1988. He became an associate professor in the Department of Electrical and Electronic Engineering of Kitami Institute of Technology in 1996. He has been a professor since 2008 in the same university. His research interests include the analysis of electromagnetic fields, acoustic fields, and optimization of microwave circuits. He received an IEEE AP-S Tokyo Chapter Young Engineer Award in 1992. He is a coauthor of the books *Handbook of Microwave Technology* (Academic Press) and *Antennas and Associated Systems for Mobile Satellite Communications* (Research Signpost). He is the chairman of technical committee on electronics simulation technology (EST), and a member of technical committee on electromagnetic theory (EMT) of IEICE. He holds a D.Eng. degree, and is a member of IEEJ and IEEE.